DOI: 10.1002/cbic.200500046

Stochasticity of Manganese Superoxide Dismutase mRNA Expression in Breast Carcinoma Cells by Molecular Beacon Imaging

Timothy J. Drake,[a] Colin D. Medley,[a] Arup Sen,[b] Richard J. Rogers,[c] and Weihong Tan*[a]

Visual and quantitative monitoring of cell-to-cell variation in the expression of manganese superoxide dismutase (MnSOD) mRNA by using novel ratiometric imaging with molecular beacons (MB) reveals a distinct change in patterns following induction of human breast-carcinoma cells with lipopolysaccharide. Interestingly, the pattern of cell-to-cell variation in a cell line stably transfected with a plasmid bearing a cDNA clone of MnSOD and overproducing the enzyme is significantly different from the pattern associated with MnSOD induction. The levels and the patterns of cell-population heterogeneity for β-actin mRNA expression do not show distinct changes either following induction or in stably transfected cells. These results are significant in light of the reported relationship between this enzyme and malignant phenotype of breast-carcinoma cells. Use of MBs in ratiometric image analyses for cytoplasmic mRNAs represents a novel means of directly examining the stochasticity of transcription of MnSOD and other genes implicated in cellular phenotype regulation.

Introduction

There is a growing realization that an "average" cell, as defined by cell population analysis,[1,2] might not exist and that stochastic effects in gene expression can play crucial roles in biological processes and cellular fates.[3–5] In situ hybridization on fixed cells might not accurately depict these events in living cells.[6] Similarly, single-cell reverse-transcriptase-PCR[7] suffers from variations in amplification between various mRNAs. Molecular beacons (MB), on the other hand, are a novel class of fluorescent biosensors for sensitive, nonradioactive monitoring of the structure and activity of genes in vitro and intracellularly (www.molecular-beacons.org).[8] MBs can be introduced into living cells and used for target detection without the need for separating the hybridized material or additional signal amplification. The use of MBs in intracellular analyses has been mostly limited to visualization and not quantitation, since the results based on single fluorescence measurements are complicated by signal changes from light scattering by the sample, excitation source fluctuations, and variability in the intracellular delivery and trafficking of MB molecules.[8,9] Ratiometric determinations[10,11] compensate for the variability by taking the ratio of the signal intensity from the specific probe for a target over the signal produced by a control unrelated probe that serves as the reference.

Real-time visualization and quantitation of changes in cytoplasmic mRNA levels of genes that are involved in pathways implicated in tumorigenesis and the identification of shift in cell subpopulations should provide valuable insights into understanding the impact of intracellular changes associated with the progression of cancer. We used MBs in a novel ratiometric fluorescence-imaging method to monitor cytoplasmic mRNA levels of manganese superoxide dismutase (MnSOD), an enzyme that regulates cellular levels of reactive oxygen species (ROS) and is implicated in malignant the phenotype of tumor cells.[12] The tumor-suppressive effects of MnSOD, including a polymorphic variant of the enzyme with a higher specific activity in suppressing the invasiveness of tumors, have been reported.[13] Monitoring cell-to-cell variation in populations of different breast-carcinoma cell lines could yield important information on the potential effects of the stochasticity of MnSOD transcription on variations in the levels of ROS and the malignant phenotype of breast-cancer cells. Our ratiometric-image analyses were performed on the cytoplasm following microinjection of a gene-specific MB admixed with an excess of a heterologous DNA labeled with a matching fluorophore that had the same emission but a different excitation spectrum. This method showed significantly less inherent experimental variation than those reported for other fluorescence-imaging approaches with DNA probes. We observed both an increase and

[a] *T. J. Drake, C. D. Medley, Prof. W. Tan*
Center for Research at the Bio/Nano Interface
Department of Chemistry, Shands Cancer Center, UF Genetics Institute
and McKnight Brain Institute, University of Florida
Gainesville, FL 32611 (USA)
Fax: (+1) 352-846-2410
E-mail: tan@chem.ufl.edu

[b] *A. Sen*
GenoMechanix, L. L. C.
2444 NE 1st Blvd. Suite 800
Gainesville, FL 32609 (USA)

[c] *R. J. Rogers*
Department of Anesthesiology
University of Florida College of Medicine
Gainesville, FL 32610 (USA)

changes in the profile of cell-to-cell variation in MnSOD mRNA expression in an MDA-MB-231 breast-carcinoma cell line within 4 h after lipopolysaccharide (LPS) treatment to induce the MnSOD enzyme; this is consistent with previous LPS-induction experiments.[14] An MCF-7 breast-carcinoma cell line that is stably transfected with an MnSOD cDNA clone, and thus overexpresses the MnSOD enzyme, showed a different pattern of cell-to-cell variation in cytoplasmic MnSOD mRNA than the pattern associated with LPS-induced overproduction. The basal profile of cell-to-cell variation observed with a MB for β-actin mRNA was distinct from that of MnSOD in each cell line and did not detectably change following LPS treatment. The use of MBs to visualize and monitor changes in profiles of cell-to-cell variation of cytoplasmic mRNA in cell lines provides new information on the effects of MnSOD mRNA expression on the phenotypes of breast-carcinoma cells.

Results and Discussion

A major issue with using MBs for intracellular mRNA measurements is the inherent experimental variability associated with the delivery of extremely small volumes of MB solutions into cells. As a result, observed differences between individual cells do not reflect actual cell-to-cell variation of the targets being monitored,[8] especially since minimal variations in the injected volumes result in large deviations in the measured fluorescence intensity. We, therefore, utilized a mixture of the gene-specific MB with a fluorophore-matched reference DNA as described below.

Development and validation of the ratiometric imaging with MBs in breast-carcinoma cells in culture

We first evaluated the robustness of our novel ratiometric method using a test target sequence (5′-GCGACCATAGCGATTTAGA-3′) introduced into a MDA-MB-231 breast-carcinoma cell line by microinjection, followed by the application of the test MB-1 and scramble sequence mixture (1 μM MB-1 and 10 μM RuBpy-labeled scrambled DNA; MB-1: 5′-CCTAGCTC-TAAATCGCTATGGTCGCGCTAGG-3′; scrambled DNA: 5′-TCGCGTGCGTGACACATCGACATCTCGTGTA-3′). Our choice of Texas Red and RuBpy as the matching fluorophores for the MBs and the heterologous DNA, respectively, was based on the fact that the fluorescence excitation of RuBpy does not overlap with the excitation of Texas Red. Also, their emissions are similar due to the large Stokes shift of RuBpy. This allows us to utilize a high-speed monochromator-based imaging system without the need to switch emission filters.

The predicted theoretical ratio enhancement in response to an MB is the ratio of specific signals between the "open" (when the target hybridizes to the MB loop) and the "closed" (when the stem of the MB is intact) states of the MB. We microinjected solutions of "closed" and "open" MB (created by adding an excess of test target to an MB solution) mixed with the reference RuBpy-labeled heterologous DNA, and determined that the ratio enhancement was ~2.6-fold intracellularly. This ratiometric enhancement value was very consistent from cell-to-cell.

In order to mimic the practical intracellular conditions under which the MB loop would recognize its complementary target sequence embedded in a longer sequence, we microinjected a 140-mer DNA, designated DNA-140T and which contained the test target, and a 154-mer of unrelated DNA, designated DNA-154C, without the test target sequence, in MDA-MB-231 cells. Subsequent microinjection of the MB-scrambled DNA mixture produced a ratiometric response of approximately 0.62 in cells that received DNA-140T, while the DNA-154C control and the blank (i.e. buffer injection) produced no detectable change ($R = 0.27$ and 0.23, respectively, Figure 1 A).

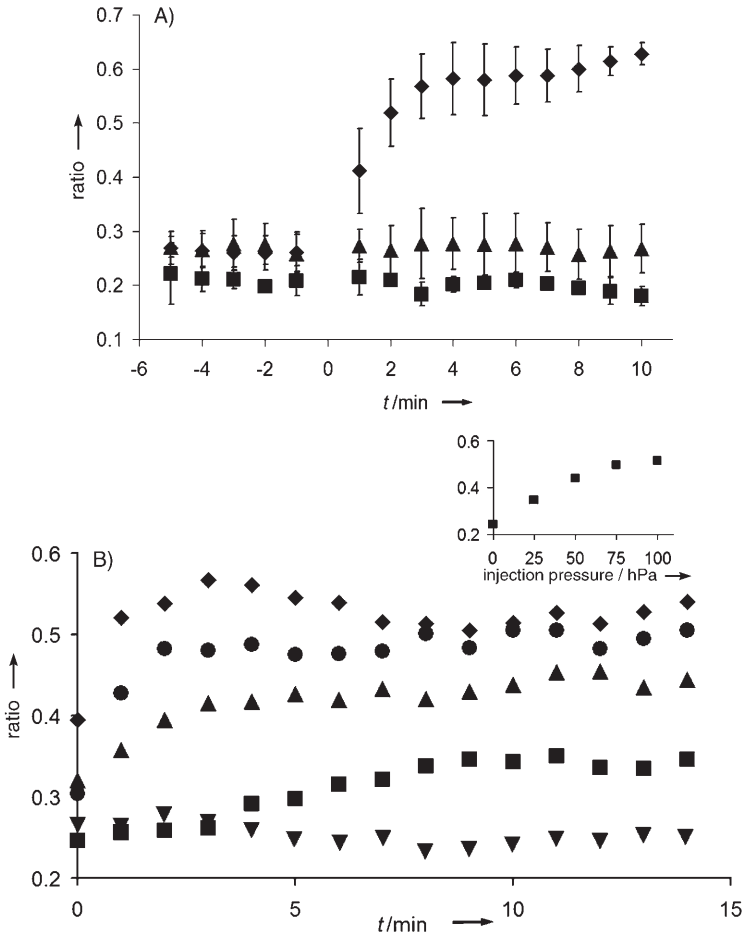

Figure 1. Ratiometric values for A) long synthetic DNA-140T (◆) and DNA-154C (■), and the blank microinjection buffer (▲). B) Various amounts of DNA-140T injected in human breast-carcinoma cells by changing the sample injection pressure: (◆) 100 hPa, (●) 75 hPa, (▲) 50 hPa, (■) 25 hPa, and (▼) control. Dual microinjections were performed as described in the Experimental Section. Ratiometric image collection and data analysis were performed as described above. The inset shows the ratiometric response versus the sample injection pressure. A clear dose dependence is observed, with saturation occurring at 75–100 hPa.

We next tested the ability of microinjected MB to distinguish between different levels of expression inside the cells. To simulate varying concentrations of intracellular targets, a 1 μM DNA-140T solution was first injection into the cell at varying pressures by using the microinjector's injection-pressure controls (Figure 1B). As a result of varying the pressure, different volumes of solution were delivered to the cell and, consequently, varying amounts of the target. Once the target had been injected, a probe solution containing 1 μM MB-1 and 10 μM RuBpy-labeled scramble DNA was microinjected at 50 hPa. Based on the averages of the ratiometric values between 10 and 15 min, a clear concentration-dependent response was observed (Figure 1B inset). Although our results show that the ratiometric values are clearly proportional to the levels of mRNA, technical difficulty in delivering precisely measured amounts of the test target limits our ability to determine the absolute amount of a target from the ratiometric value.

Monitoring cytoplasmic MnSOD mRNA in breast-carcinoma cells in culture

The MDA-MB-231 human cell line used in this report expresses reasonable levels of the mRNA, and the levels of expression of this mRNA are known to be regulated in response to certain mediators of cellular inflammatory response.[14,15] A number of MBs were designed to recognize different portions of the human MnSOD mRNA sequence (GenBank Accession No. NM-000636) and tested in the in vitro fluorescent enhancement assay (as described in the Experimental Section) with synthetic target DNAs that are complementary to the loop sequences of the MBs. A single injection of 1 μM MB-2 (5′-CCGAGCCAGTTA-CATTCTCCCAGTTGATTGCTCGG-3′) and 10 μM RuBpy-labeled scramble DNA was performed in individual cells. Unlike the test system described above for microinjected exogenous target, MnSOD mRNA is present in the cell cytoplasm at the time of injection. As a result, the ratiometric response does not start at a closed ratiometric value and this is observed due to the amount of time that elapses between performing the injection and starting the acquisition of images. Figure 2A depicts a typical ratiometric image response from individual cells. In Figure 2B, MB-1 intracellular responses are constant and stable throughout the time course of the experiment. The results of ratiometric values shown in Figure 2A and images shown in C clearly indicate cell-to-cell variation in endogenous levels of the message. Our observation was consistent with other findings from fixed cells in which the expression profiles of genes vary significantly from cell to cell in a population.[3–5]

Ratiometric imaging of cell-to-cell variation profiles of MnSOD mRNA expression in breast-carcinoma cells in culture before and after LPS induction

Perhaps the most remarkable characteristic of MnSOD is its ability to up-regulate in response to a variety of inflammatory stimuli and cellular stress. Expression of MnSOD also causes significant alterations in the malignant phenotype as well as inhibition of tumor growth in vivo.[16,17] Here, MDA-MB-231

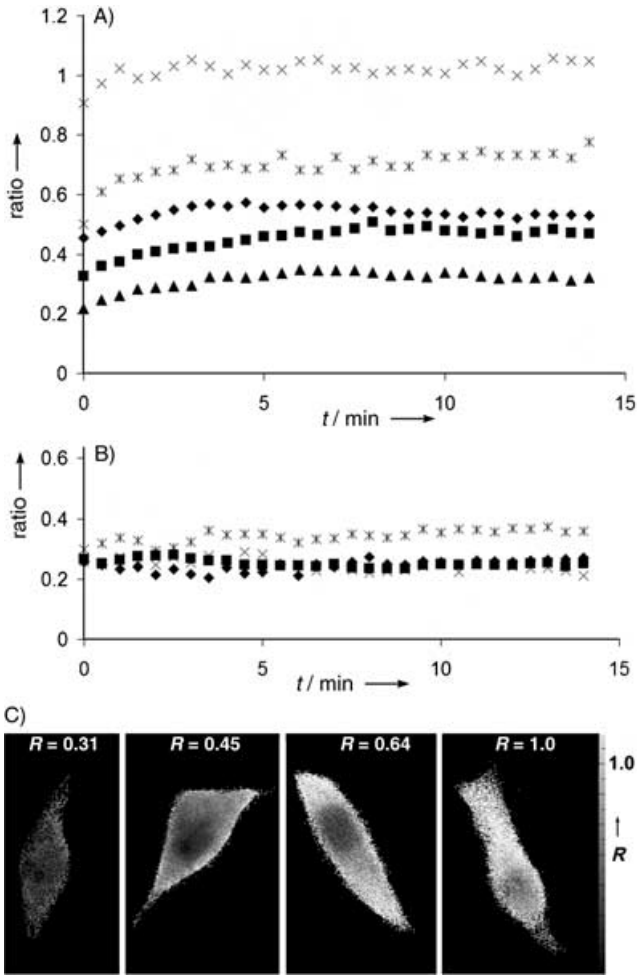

Figure 2. Ratiometric values for MDA-MB-231 cells A) with MB-2 for human MnSOD mRNA, and B) with control molecular beacon MB-1 for Test Target. C) Ratiometric images of MDA-MB-231 cells at 10 min after the injection of MB-2. *R* values indicate the average ratiometric value of the cytoplasm after analysis as described in the Experimental Section.

cells were used to determine profiles of cell-to-cell variation in MnSOD mRNA expression before and after treatment with LPS. These cells express easily detectable levels of the MnSOD mRNA as shown by Northern analysis (Figure 3A). Based on the ability of these cells to produce a noticeable change in mRNA expression after 4 h of incubation with 0.5 μg mL^{-1} LPS,[14] single-cell expression profiles were determined by microinjecting 1 μM MB-2- and 10 μM RuBpy-labeled scramble DNA. For a MB probe control, 1 μM MB-1- and 10 μM RuBpy-labeled scramble DNA was microinjected to determine if there was any nonspecific opening of the MB in LPS-induced cells. As a biological control, an MB (designated MB-3; 5′-CCGTCGAGGAAGGAAGGCTGGAAGAGCGACGG-3′) for the detection of human β-actin mRNA was microinjected with the scramble DNA. In all cases, ratiometric images were acquired for 15 minutes at intervals of 1 minute. As was done for the calibration curve, frames 10–15 were averaged together to produce the response from each individual cell. Figure 3B shows that when the control MB-1 is used, there is only modest cell-to-cell variation, and LPS induction shows little or no change

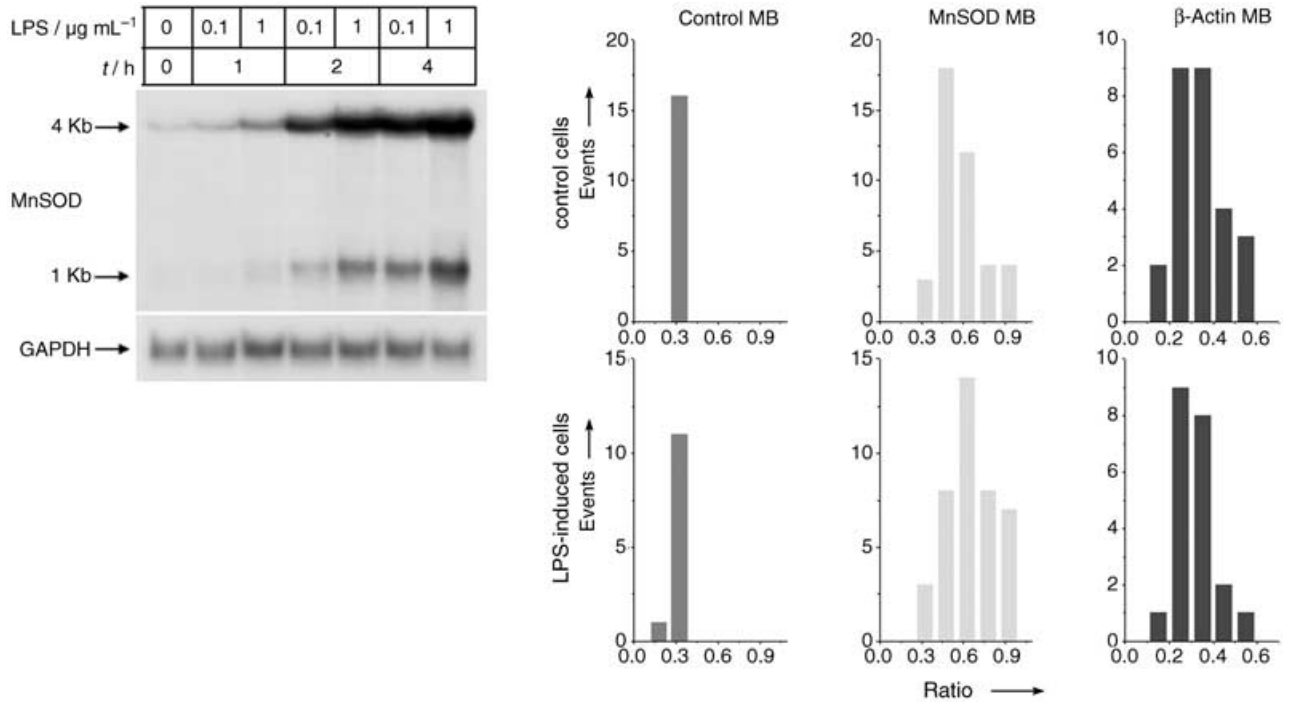

Figure 3. Analysis of LPS-induced MDA-MB-231 cells. A) Northern analysis of LPS-induced cells. B) Histograms showing the distribution of ratiometric responses for control and LPS-induced cells with control MB-1 for the test target, MB-2 for MnSOD and MB-3 for β-actin.

in the histogram of cell distribution (preinduction: average ratiometric value = 0.31 ± 0.05, skew = −0.17; postinduction: average ratiometric value = 0.27 ± 0.04, skew = 0.60). For the β-actin control, again no shift was observed (preinduction: average ratiometric value = 0.36 ± 0.1, skew = 0.61; postinduction: average ratiometric value = 0.32 ± 0.1, skew = 0.77). However, the histogram for MnSOD expression levels obtained with MB-2 shows a very different cell-to-cell variation even prior to any treatment with LPS. A peak ratiometric value from the histogram occurred in the bin for 0.40 to 0.55. The average expression level corresponds to 0.57 ± 0.17 with a skew of 0.9. At approximately 4 hours after LPS induction, the histogram shows that the peak ratiometric value shifted to bin 0.55 to 0.70. The average expression level corresponds to 0.66 ± 0.18 with a skew of 0.3. This shift is consistent with the increase in mRNA determined by Northern analysis. We also observed a significant rise in cells that overexpress MnSOD mRNA after 4 h of LPS induction, as indicated by a near doubling of the number of cells in the bin 0.70–1.0. This is the first description of living single-cell expression analysis of MnSOD mRNA in breast-carcinoma cells that clearly show a general shift to the right, consistent with increased expression, while also detecting a small fraction of cells that show very high expression levels following LPS induction. The ability to identify cells in a population with significantly higher levels of MnSOD mRNA expression may be valuable in comparing cell-to-cell stochasticity in breast-carcinoma cell lines that display different malignant phenotypes.

Cell-to-cell variation profiles of MnSOD mRNA expression in breast-carcinoma cells with distinct malignant phenotypes

We next used our ratiometric imaging approach to monitor the cell-to-cell variation in MnSOD mRNA expression patterns in an MCF-7 cell line that had been stably transfected to overexpress the MnSOD gene and that displayed a less malignant phenotype.[18] The transfected MCF-7 cell line, SOD50, was a kind gift from the laboratory of Dr. Larry Oberley, University of Iowa.[13,18] Ratiometric distribution profiles were determined for both MB-2 and MB-3 in these cells (Figure 4A). To distinguish between cell populations, each cellular response was monitored, and the final five images for each excitation wavelength were averaged and plotted as a function of the 575 nm excitation fluorescence signal versus the 450 nm excitation fluorescence signal (Figure 4B and C). With MB-3 for β-actin, no significant difference is observed between the three cell populations analyzed. In contrast3, noticeable changes in the MnSOD expression patterns levels are observed between the cell populations. The slopes of the fitted lines for each induction response corresponded to the average ratiometric response for the cell populations analyzed. In Figure 4B, the basal β-actin response was 0.36 while the LPS-induced and MnSOD overexpressed cells were 0.32 and 0.39, respectively. In Figure 4C, the basal MnSOD response was 0.57 while the LPS-induced and MnSOD overexpressed cells were 0.66 and 0.85, respectively.

The results of cell-to-cell variation in MnSOD mRNA expression obtained with the novel ratiometric imaging approach might be significant in that malignant phenotype of MCF-7 breast-carcinoma cells might be governed by both mRNA expression and enzyme activity (such as in the Ile58 polymorphic

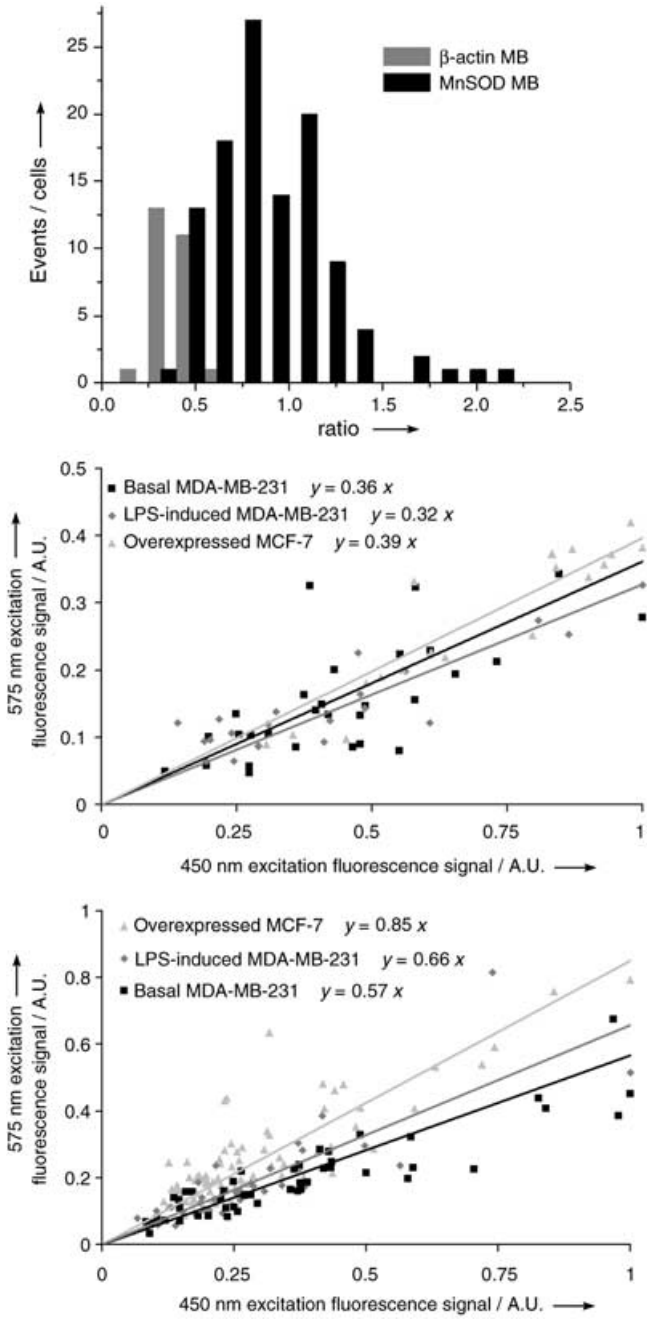

Figure 4. Histogram and scatter plot analysis of ratiometric single cell responses. A) Histogram showing the distribution profile of MB-2 and MB-3 ratiometric responses for MnSOD overexpressing MCF-7 cells. B) MB-3 for β-actin mRNA detection for noninduced MDA-MB-231 cells, LPS-induced MDA-MB-231 cells, and MnSOD overexpressing MCF-7 cells. C) MB-2 for MnSOD mRNA detection for noninduced MDA-MB-231 cells, LPS-induced MDA-MB-231 cells, and MnSOD overexpressing MCF-7 cells. Each scatter is linearly fitted to determine the ratiometric response for each cell population.

variant described by Zhang et al.).[13] The difference in the patterns (Figure 3 and Figure 4A) of cell-to-cell variation we observed is consistent with the assumption that stochastic effects in the expression of a chromosomal gene in response to an external stimulus, such as LPS induction, are different from those involved in the expression of an exogenously introduced autosomal gene.[3–5] The methodology described here incorporates the microinjection of MB probes. As a result, the microinjection process and presence of the probes could potentially have an impact on our results. However, since the control MB response for injection of targets with varying amounts did not reveal any adverse affects on the MB function—the induced and overexpressed MnSOD systems show clear differences in the populations, and the β-actin MB shows no clear differences in the populations before and affect induction—the adverse effects that are possible are minimal in the system analyzed. Future studies along these lines might provide new insights and strategies into studying the efficacy of drugs at the level of gene transcription and of gene constructs used in gene therapy.

MnSOD has been implicated in the malignant phenotype of tumor cell lines, presumably through a pathway that affects the production of matrix metalloproteinases and changes in intracellular levels of ROS.[16–18] Our results with the MDA-MB-231 breast-carcinoma cell line show distinct patterns of cell-to-cell variation for MnSOD mRNA and β-actin mRNA. We also observed that LPS induction caused a clear "right" shift in the cell-subpopulation profile that indicates elevated MnSOD mRNA expression across the entire cell population, while no such shift was detected for β-actin mRNA. An MCF-7 breast-carcinoma cell line stably transfected with an MnSOD cDNA plasmid to constitutively overexpress MnSOD displayed a different profile of cell subpopulations with significantly more cells expressing higher levels of MnSOD mRNA. No such distribution change in cell subpopulation was observed for β-actin mRNA.

Conclusion

The underlying cause or the functional consequence of heterogeneity observed in the expression of a single gene among individual cells in a population is not well understood. However, it is recognized that the inherent stochasticity of the biochemical processes involved in gene expression and the response to fluctuations in extracellular and intracellular components contribute to such cell-to-cell variations.[3–5] Heterogeneity in the expression of various tumor antigens in cells within a single nodule is well recognized and remains a challenge in the development of targeted cancer therapy, especially for solid tumors. Systematic studies that monitor the expression of regulatory and housekeeping genes with respect to the basal heterogeneity and changes associated with a disease process, or in response to a biological modifier, are likely to provide new insights into the regulation of cellular phenotypes.

Our studies support the notion that the reported effects of MnSOD on the malignant phenotype of tumor cells might, at least in part, be working in individual cells through changes in the levels of mRNA and not by cell-to cell communication by which cells producing higher levels of the enzyme affect other cells in a population. Additional experiments with this novel fluorescence-based intracellular imaging with MnSOD mutations that alter the specific activity of the encoded enzyme will be useful in further delineating the regulation of MnSOD gene

expression and the regulation of malignant phenotypes in individual cells in a population.

The ratiometric imaging method used here could also have broad applications extending the use of MBs to monitor changes in cell-to-cell variation in the expression of other cis- and trans-acting genes associated with changes in the phenotype at the level of single cells in a population. This ratiometric fluorescence-imaging approach to identifying profiles of cell subpopulations with different levels of intracellular mRNA parallels the fluorescence-activated cell sorting used in studying the expression of cell-surface proteins in living cells. Since MnSOD is implicated in the regulation of cellular phenotypes in many other diseases, ratiometric analysis with the MnSOD MB in other cell lines might provide new information on the relevance of stochastic effects in MnSOD transcription in other disease processes.

Experimental Section

All chemicals and solvents were purchased from Sigma (St. Louis, MI), unless stated otherwise, and used without additional purification. RuBpy was purchased from Sigma, the Texas Red NHS ester was purchased from Molecular Probes (Eugene, OR), and controlled-pore glass resins and phosphoramidites for DNA and RNA synthesis were purchased from Biosearch Technologies, Inc. (Novato, CA) and Transgenomics (Omaha, NE). The human breast-carcinoma cell line MDA-MB-231 (ATCC Catalogue No. HTB-26) was purchased from American Type Culture Collection (Manassas, VA).

Molecular beacon, reference probe, and DNA synthesis: Synthetic DNAs, including MBs, and RNAs were produced by using the standard phosphoramidite chemistry in Perseptive Biosystems 8909 automated synthesizers, deprotected with ammonium hydroxide or methanolic potassium carbonate, and purified by using reversed-phase or ion-exchange HPLC. Fluorophore labeling of synthetic DNA and RNA with Texas Red and RuBpy dyes was done by using the succinimidyl ester of the respective fluorophore to react with a functional amino group on the desired end of the DNA or RNA. Synthesis of MBs was carried out by using BHQ2 quencher immobilized on controlled-pore glass resin to label the 3′-end and adding a functional amino-group modifier at the 5′-end. Subsequent to purification, the succinimidyl ester of Texas Red was used to couple the fluorophore. Final labeled DNA, RNA, and MB were purified by multiple rounds of reversed-phase HPLC purification by using acetonitrile with triethyl amine acetate (0.1 M, pH 6.0) as the mobile phase. All synthetic DNA and RNA preparations were stored in sterile R.O. water (treated with diethyl pyrocarbonate for use in storing RNAs) at −20 °C until use.

Instrument setup, cell culture, and microinjections: Fluorescence imaging was performed with an inverted fluorescence microscope (Olympus, CSquared Corp., Tamarac, FL). The excitation light source was a TILL-Phontics high-speed monochromator-based imaging system equipped with a high quantum efficiency monochrome charge-coupled device (CCD; Applied Scientific Instrumentation, Eugene, OR). Cellular images were conducted with an oil immersion 40X, N.A. 1.35 objective. This setup allows for ratiometric imaging in the form of dual-excitation and single-emission detection. As a result, RuBpy, which has an excitation maximum at 450 nm and an emission maximum at 620 nm, can be excited and detected with minimal overlap in excitation from Texas Red, which has an excitation maximum at 595 nm and an emission maximum at 615 nm. The filter cube used in these studies was purchased from Omega Optics (Brattleboro, VT) and allowed for both 450 nm and 575 nm to be reflected to the sample and 615 nm light to be transmitted to the detector. 575 nm was chosen for the excitation of the Texas Red because the dichroic mirror transmitted too much of 595 nm light to allow for efficient detection of Texas Red.

MDA-MB-231 cells were maintained in Dulbecco's Modification of Eagle's Medium (DMEM, Fisher Scientific, Hampton, NH) supplemented with fetal bovine serum (10%. Invitrogen, Carlsbad, CA) and Gentamycin (Sigma) in T75 Falcon flasks (Fisher Scientific) in a humidified cell-culture incubator (37 °C, Revco, Asheville, NC) in CO_2 (5%). MCF-7 cells were maintained in minimal essential medium supplemented with fetal bovine serum (10%), nonessential amino acids, sodium pyruvate, and G-418 (Sigma). The cells were plated in 35 mm glass bottom culture dishes (MatTek Corp., Ashland, MA) at approximately 6×10^5 cells per dish 48 h prior to use for microinjection. To maintain cell viability during microinjection and manipulation, a cell-culture incubator was used (Harvard Apparatus, Holliston, MA) to maintain temperature and humidity. Probe solutions for microinjection were freshly prepared by mixing Texas Red-labeled DNA (or a MB) with the control RuBpy-labeled DNA (1 μM and 20 μM, respectively in 20 mM Tris, pH 7.4, 50 mM NaCl, and 5 mM $MgCl_2$ buffer). Similarly, all sample solutions were prepared with the microinjection buffer. An Eppendorf microinjection system (Brinkman, Westbury, NY) and Burleigh micromanipulators (EXFO Burleigh Products Group Inc., Victor, NY) were used to carry out the delivery of MB probe solutions to the cells. All microinjections were done by positioning an Eppendorf Femtotip I (Brinkman) inside the cytoplasm of a single cell. Fluorescence images were acquired by first exciting the microinjected cells at 450 nm to excite the RuBpy dye for 500 ms and simultaneously capturing the fluorescence with the CCD camera for 500 ms. After a 3 ms delay, the cells were excited at 575 nm to excite Texas Red for 500 ms while simultaneously capturing the fluorescence emission with the CCD camera for 500 ms. This process was repeated throughout the time course of the experiment at 1 min intervals.

Dynamic measurements for heterologous nucleic acid targets introduced in the cells were carried out by using two injections. The first, called "probe injection", was a mixture of MB-1 with the RuBpy-labeled reference DNA solution, and the second was the test target nucleic acid solution. After the first injection, fluorescence images for both fluorophores were monitored for 5 min to obtain the background ratio value expected for the MB in its "closed" conformation. The second, called the "sample injection", was then performed, and fluorescence images were acquired for an additional 10 min.

Data analysis: An important part of this method is the ability to analyze two fluorescence images to produce both ratiometric images and measure fluorescence ratio enhancements produced by the MB, relative to the control probe, in response to its intracellular target. Equation (1) was used for ratiometric calculations with Texas Red and RuBpy fluorophores:

$$R = \frac{S_{\text{Texas Red}} - B_{\text{Texas Red}}}{S_{\text{RuBpy}} - B_{\text{RuBpy}}} \quad (1)$$

here R is the ratiometric value, S is the fluorescence intensity, and B is the background fluorescence intensity. For both the RuBpy and Texas Red fluorescence images, background levels were based on the signals produced when no fluorescence was observed in the images. To accomplish this, a Till-Vision software package (Applied Scientific Instrumentation) was used to select the region

around the outside of the cell, and the corresponding pixel intensities were averaged to yield the background signal (*B*). Based on the fluorescence images of Texas Red ($S_{\text{Texas Red}}$) and RuBpy (S_{RuBpy}) and the background determinations for each time point in the experiments, ratiometric images for the injection of solutions containing 1 μM Texas Red-labeled DNA (or MBs) and 20 μM RuBpy-labeled DNA were determined by dividing the fluorescence images of ($S_{\text{Texas Red}}-B_{\text{Texas Red}}$) by ($S_{\text{RuBpy}}-B_{\text{RuBpy}}$). Ratiometric values were then obtained from the ratiometric images by selecting only the cytoplasm of the cell and analyzing it with the software to determine the average ratiometric value of the pixels analyzed. Due to nuclear uptake of the DNA probes, the nucleus was omitted from the analysis. Finally, ratio enhancements were determined by normalizing the ratiometric responses of the MBs to the background ratiometric value of the MB in the absence of target nucleic acids. For the MB specific for MnSOD mRNA, ratio enhancements were determined by normalizing the MB response to the first image acquired immediately after the probe injection. It should be noted that all images presented here display assigned color representations of the fluorescence intensities and ratiometric values. As a result, the colors chosen to represent the fluorescence or ratiometric values do not correspond to the actual emission wavelengths of the fluorophores. Based on our experience, when cells are overfilled, the RuBpy signal decreases rapidly, most likely due to leakage. On the other hand, if an inadequate amount of labeled DNAs is delivered to the cell, the RuBpy signal was only 10–15 units above the background, and, accordingly, the Texas Red signal from the MB was not detectable. Based on these characteristics, the best injections for MB measurements had RuBpy signals that were approximately 90–100 units above background and maintained constant fluorescence intensity.

To examine the single-cell responses for stimulated and endogenously overexpressed MnSOD, histogram plots of the cellular events versus ratiometric value after 10 min following probe injection were created. Bin values in the histograms were set based on the response of the control MB. Since the control MB does not open inside the cell, the bin size that incorporates all the events was determined so as to obtain a single bar distribution of the ratiometric values. All probes were plotted with the same bin size. A considerable shift in the populations was also determined, based on this bin size.

In vitro fluorescence-enhancement studies: All fluorescence-enhancement measurements of MBs in vitro were carried out by incubating a solution of MB (1 μM) in Tris (20 mM, pH 7.4), NaCl (50 mM), and $MgCl_2$ (5 mM) buffer in a total volume of 20 μL with the test DNA or RNA at a tenfold molar excess. The reactions were allowed to proceed for 30 min in Corning low-volume 384-well microplates (Fisher Scientific Co., Pittsburgh, PA), and the fluorescence (575 nm excitation and 615 nm emission) was read by using a Teacan Safire monochromator-based microplate reader (Maennedorf, Switzerland). Fluorescence enhancements were calculated by using Equation (2)

$$\frac{S_{\text{openMB}}-B_{\text{openMB}}}{S_{\text{closedMB}}-B_{\text{closedMB}}} \quad (2)$$

here *S* is the average fluorescence intensity of the MB, *B* is the background intensity, "open" represents the solution to which a DNA or RNA target sample is added, and "closed" represents the solution to which nothing was added. A cDNA copy of MnSOD mRNA was produced by reverse transcription from human embryonic kidney total RNA by using Invitrogen SuperScript reverse transcriptase (Carlsbad, CA) and cloned into a PCRScript vector (Stratagene, La Jolla, CA). The cDNA sequence and orientation were verified by sequence analysis of the PCRScript vector. The in vitro MnSOD mRNA transcripts were produced by using the Ambion MEGAscript (Austin, TX) and were analyzed by Northern blot analysis with a ^{32}P probe complementary to the human MnSOD (GenBank Accession No. NM-000636).

Acknowledgements

This work was partially supported by grants from NSF NIRT, Packard Foundation and from the NIH, grants GM66137 and NS045174.

Keywords: ab initio calculations · fluorescent probes · FRET · gene expression · mRNA · nucleic acids

[1] M. Chee, R. Yang, E. Hubbell, A. Berno, Huang, C. X. D. Stern, J. Winkler, D. J. Lockhart, M. S. Morris, S. P. A. Fodor, *Science* **1996**, *274*, 610–614.
[2] D. G. Ginzinger, *Exp. Hematol.* **2002**, *30*, 503–512.
[3] M. B. Elowitz, A. J. Levine, E. D. Siggia, P. S. Swain, *Science* **2002**, *297*, 1183–1186.
[4] J. M. Levsky, R. H. Singer, *TrendsCell Biol.* **2002**, *13*, 4–6.
[5] D. E. Zak, G. E. Gonye, J. S. Schwaber, F. J. Doyle III, *Genome Res.* **2003**, *13*, 2396–2405.
[6] R. W. Dirks, C. Molenaar, H. J. Tanke, *Histochem. Cell Biol.* **2001**, *115*, 3–11.
[7] N. J. Sucher, D. L. Deitcher, D. J. Baro, R. M. Harris Warrick, E. Guenther, *Cell Tissue Res.* **2000**, *302*, 295–307.
[8] T. J. Drake, W. Tan, *Appl. Spectrosc.* **2004**, *58*, 269A–280A.
[9] J. R. Lakowicz, *Principles of Fluorescence Spectroscopy*, 2nd ed. Kluwer/Plenum, New York, **1999**; C. D. Medley, T. J. Drake, J. M. Tomasini, R. J. Rogers, Tan, W. *Anal. Chem.* **2005**, *77*, 4713.
[10] S. L. Barker, H. A. Clark, S. F. Swallen, R. Kopelman, A. W. Tsang, J. A. Swanson, *Anal. Chem.* **1999**, *71*, 1767–1772.
[11] D. P. Bratu, B. j. Cha, M. M. Mhlanga, F. R. Kramer, S. Tyagi, *Proc. Natl. Acad. Sci. USA* **2003**, *100*, 13308–13313.
[12] C. B. Ambrosone, J. L. Freudenheim, P. A. Thompson, E. Bowman, J. E. Vena, J. R. Marshall, S. Graham, R. Laughlin, T. Nemoto, P. G. Shields, *Cancer Res.* **1999**, *59*, 602–606.
[13] H. J. Zhang, T. Yan, T. D. Oberley, L. W. Oberley, *Cancer Res.* **1999**, *59*, 6276–6283.
[14] G. A. Visner, W. C. Dougall, J. M. Wilson, I. A. Burr, H. S. Nick, *J. Biol. Chem.* **1990**, *265*, 2856–2864.
[15] K. Mitrunen, P. Sillanpää, V. Kataja, M. Eskelinen, V. M. Kosma, S. Benhamou, M. Uusitupa, A. Hirvonen, *Carcinogenesis* **2001**, *22*, 827–829.
[16] J. J. Li, L. W. Oberley, D. K. St. Clair, L. A. Ridnour, T. D. Oberley, *Oncogene* **1995**, *10*, 1989–2000.
[17] T. Yan, L. W. Oberley, W. Zhong, D. K. St. Clair, *Cancer Res.* **1996**, *56*, 2864–2871.
[18] H. J. Zhang, W. Zhao, S. Venkataraman, M. E. C. Robbins, G. R. Buettner, K. C. Kregel, L. W. Oberley, *J. Biol. Chem.* **2002**, *277*, 20919–20926.

Received: February 1, 2005
Revised: June 14, 2005
Published online on October 4, 2005

